

# Computer Implementation of the Drbem for Studying the Generalized Thermoelastic Responses of Functionally Graded Anisotropic Rotating Plates with One Relaxation Time

**M. A. Fahmy**

Mathematics Department, University College, Umm Al-Qura University, Makkah  
The Kingdom of Saudi Arabia.  
Faculty of Computers and Informatics, Suez Canal University  
Ismailia, Egypt.

**A. M. Salem**

Faculty of Computers and Informatics  
Suez Canal University  
Ismailia, Egypt.

**M. S. Metwally**

**M. M. Rashid**

Faculty of Science  
Suez University  
Suez, Egypt.

## Abstract

*A numerical computer model based on the dual reciprocity boundary element method (DRBEM) is extended to study the generalized thermoelastic responses of functionally graded anisotropic rotating plates. In the case of plane deformation, a predictor-corrector implicit-explicit time integration algorithm was developed and implemented for use with the DRBEM to obtain the solution for the displacement and temperature fields in the context of the Lord and Shulman theory. Numerical results that demonstrate the validity of the proposed method are also presented in the tables.*

**2010 Mathematics subject classification:** 74B05 74E05 74F05 74H05 74S20

**Key words:** Thermoelasticity; Rotation; Functionally graded Material; Anisotropic; Dual Reciprocity Boundary Element Method.

## 1. Introduction

Biot [1] introduced the classical coupled thermo-elasticity theory (CCTE) to overcome the first shortcoming in the classical thermo-elasticity theory (CTE) introduced by Duhamel [2] and Neuman [3] where it predicts two phenomena not compatible with physical observations. First, the equation of heat conduction of this theory does not contain any elastic terms. Second, the heat equation is of a parabolic type, predicting infinite speeds of propagation for heat waves. Most of the approaches that came out to overcome the unacceptable prediction of the classical theory are based on the general notion of relaxing the heat flux in the classical Fourier heat conduction equation, thereby introducing a non-Fourier effect. One of the simplest forms of these equation is due to the work of Lord and Shulman [4] who introduced extended thermo-elasticity theory (ETE) with one relaxation time by constructing a new law of heat conduction to replace the classical Fourier's law. This law contains the heat flux vector as well as its time derivative. It contains also new constant that acts as relaxation time. Since the heat equation of this theory is of the wave-type, it automatically ensures finite speeds of propagation for heat and elastic waves. Green and Lindsay [5] included a temperature rate among the constitutive variables to develop a temperature-rate-dependent thermo-elasticity theory (TRDTE) that does not violate the classical Fourier's law of heat conduction when the body under consideration has a center of symmetry; this theory also predicts a finite speed of heat propagation and is known as the theory of thermoelasticity with two relaxation times.

According to these theories, heat propagation should be viewed as a wave phenomenon rather than diffusion one. Relevant theoretical developments on the subject were made by Green and Naghdi [6, 7] they developed three models for generalized thermoelasticity of homogeneous isotropic materials which are labeled as model I, II and III. It is hard to find the analytical solution of a problem in a general case, therefore, an important number of engineering and mathematical papers devoted to the numerical solution have studied the overall behavior of such materials (see, e.g., [8-27]).

Functionally graded materials (FGMs) are made of a mixture with arbitrary composition of two different materials, and the volume fraction of each material changes continuously and gradually. The FGMs concept is applicable to many industrial fields such as aerospace, nuclear energy, chemical plant, electronics, biomaterials and so on. Works by Skouras et al. [28], Mojdehi et al. [29], Loghman et al. [30] and Mirzaei and Dehghan [31] are examples involving functionally graded materials.

One of the most frequently used techniques for converting the domain integral into a boundary one is the so-called dual reciprocity boundary element method (DRBEM). This method was initially developed by Nardini and Brebbia [32] in the context of two-dimensional (2D) elastodynamics and has been extended to deal with a variety of problems wherein the domain integral may account for linear-nonlinear static-dynamic effects. A more extensive historical review and applications of dual reciprocity boundary element method may be found in Brebbia et al. [33], Wrobel and Brebbia [34], Partridge and Brebbia [35], Partridge and Wrobel [36] and Fahmy [37-40].

The main objective of this paper is to study the generalized thermoelasticity problems in a rotating anisotropic functionally graded plate in the context of the Lord and Shulman theory. A predictor-corrector implicit-explicit time integration algorithm was developed and implemented for use with the dual reciprocity boundary element method (DRBEM) to obtain the solution for the temperature and displacement fields. The accuracy of the proposed method was examined and confirmed by comparing the obtained results with those known before.

## 2. Formulation of the Problem

Consider a Cartesian coordinates system  $Oxyz$  as shown in Fig. 1. We shall consider a functionally graded anisotropic plate rotating about it with a constant angular velocity. The plate occupies the region  $R = \{(x, y, z): 0 < x < \underline{\gamma}, 0 < y < \underline{\beta}, 0 < z < \underline{\alpha}\}$  with graded material properties in the thickness direction.

In this paper, the material is functionally graded along the  $Ox$  direction. Thus, the governing equations of generalized thermo-elasticity in the context of the Lord and Shulman theory can be written in the following form:

$$\sigma_{ab,b} - \rho(x+1)^m \omega^2 x_a = \rho(x+1)^m \ddot{u}_a, \quad (1)$$

$$\sigma_{ab} = (x+1)^m [C_{abfg} u_{f,g} - \beta_{ab}(T - T_0)], \quad (2)$$

$$k_{ab} T_{,ab} = \beta_{ab} T_0 [\dot{u}_{a,b} + \tau_1 \ddot{u}_{a,b}] + \rho c (x+1)^m [\dot{T} + \tau_1 \ddot{T}], \quad (3)$$

where  $\sigma_{ab}$  is the mechanical stress tensor,  $u_k$  is the displacement,  $T$  is the temperature,  $C_{abfg}$  and  $\beta_{ab}$  are respectively, the constant elastic moduli and stress-temperature coefficients of the anisotropic medium,  $\omega$  is the uniform angular velocity,  $k_{ab}$  are the thermal conductivity coefficients satisfying the symmetry relation  $k_{ab} = k_{ba}$  and the strict inequality  $(k_{12})^2 - k_{11}k_{22} < 0$  holds at all points in the medium,  $\rho$  is the density,  $c$  is the specific heat capacity,  $\tau$  is the time, and  $\tau_1$  is the mechanical relaxation time.

## 3. Numerical Implementation

Making use of (2), we can write (1) as follows

$$L_{gb} u_f = \rho \ddot{u}_a - (D_a T + \Lambda D_{a1f} u_f - \rho \omega^2 x_a) = f_{gb}, \quad (4)$$

where

$$L_{gb} = D_{abf} \frac{\partial}{\partial x_b}, D_{abf} = C_{abfg} \varepsilon, \varepsilon = \frac{\partial}{\partial x_g}, \Lambda = \frac{m}{x+1},$$

$$D_a = -\beta_{ab} \left( \frac{\partial}{\partial x_b} + \delta_{b1} \Lambda \right), f_{gb} = \rho \ddot{u}_a - (D_a T + \Lambda D_{a1f} u_f - \rho \omega^2 x_a).$$

The field equations can now be written in operator form as follows

$$L_{gb} u_f = f_{gb}, \quad (5)$$

$$L_{ab} T = f_{ab}, \quad (6)$$

where the operators  $L_{gb}$  and  $f_{gb}$  are defined in equation (4), and the operators  $L_{ab}$  and  $f_{ab}$  are defined as follows

$$L_{ab} = k_{ab} \frac{\partial}{\partial x_a} \frac{\partial}{\partial x_b}, \tag{7}$$

$$f_{ab} = \rho c(x + 1)^m [\dot{T} + \tau_1 \ddot{T}] + \beta_{ab} T_0 \dot{u}_{a,b}. \tag{8}$$

Using the weighted residual method (WRM), the differential equation (5) is transformed into an integral equation

$$\int_R (L_{gb} u_f - f_{gb}) u_{da}^* dR = 0. \tag{9}$$

Now, we choose the fundamental solution  $u_{df}^*$  as weighting function as follows

$$L_{gb} u_{df}^* = -\delta_{ad} \delta(x, \xi). \tag{10}$$

The corresponding traction field can be written as

$$t_{da}^* = C_{abfg} u_{df,g}^* n_b. \tag{11}$$

The thermoelastic traction vector can be written as follows

$$t_a = \frac{\bar{t}_a}{(x + 1)^m} = (C_{abfg} u_{f,g} - \beta_{ab}(T - T_0)) n_b. \tag{12}$$

Applying integration by parts to (9) using the sifting property of the Dirac distribution, with (10) and (12), we can write the following elastic integral representation formula

$$u_d(\xi) = \int_C (u_{da}^* t_a - t_{da}^* u_a + u_{da}^* \beta_{ab} T n_b) dC - \int_R f_{gb} u_{da}^* dR. \tag{13}$$

The fundamental solution  $T^*$  of the thermal operator  $L_{ab}$ , defined by

$$L_{ab} T^* = -\delta(x, \xi). \tag{14}$$

By implementing the WRM and integration by parts, the differential equation (6) is transformed into the thermal reciprocity equation

$$\int_R (L_{ab} T T^* - L_{ab} T^* T) dR = \int_C (q^* T - q T^*) dC, \tag{15}$$

where the heat fluxes are independent of the elastic field and can be expressed as follows:

$$q = -k_{ab} T_{,b} n_a, \tag{16}$$

$$q^* = -k_{ab} T_{,b}^* n_a. \tag{17}$$

By the use of sifting property, we obtain from (16) the thermal integral representation formula

$$T(\xi) = \int_C (q^* T - q T^*) dC - \int_R f_{ab} T^* dR. \tag{18}$$

The integral representation formulae of elastic and thermal fields (13) and (18) can be combined to form a single equation as follows

$$\begin{bmatrix} u_d(\xi) \\ T(\xi) \end{bmatrix} = \int_C \left\{ - \begin{bmatrix} t_{da}^* & -u_{da}^* \beta_{ab} n_b \\ 0 & -q^* \end{bmatrix} \begin{bmatrix} u_a \\ T \end{bmatrix} + \begin{bmatrix} u_{da}^* & 0 \\ 0 & -T^* \end{bmatrix} \begin{bmatrix} t_a \\ q \end{bmatrix} \right\} dC - \int_R \begin{bmatrix} u_{da}^* & 0 \\ 0 & -T^* \end{bmatrix} \begin{bmatrix} f_{gb} \\ -f_{ab} \end{bmatrix} dR. \tag{19}$$

It is convenient to use the contracted notation to introduce generalized thermoelastic vectors and tensors, which contain corresponding elastic and thermal variables as follows:

$$U_A = \begin{cases} u_a & a = A = 1, 2, 3; \\ T & A = 4, \end{cases} \quad (20)$$

$$T_A = \begin{cases} t_a & a = A = 1, 2, 3; \\ q & A = 4, \end{cases} \quad (21)$$

$$U_{DA}^* = \begin{cases} u_{da}^* & d = D = 1, 2, 3; a = A = 1, 2, 3; \\ 0 & d = D = 1, 2, 3; A = 4; \\ 0 & D = 4; a = A = 1, 2, 3; \\ -T^* & D = 4; A = 4, \end{cases} \quad (22)$$

$$\tilde{T}_{DA}^* = \begin{cases} t_{da}^* & d = D = 1, 2, 3; a = A = 1, 2, 3; \\ -\tilde{u}_d^* & d = D = 1, 2, 3; A = 4; \\ 0 & D = 4; a = A = 1, 2, 3; \\ -q^* & D = 4; A = 4, \end{cases} \quad (23)$$

$$\tilde{u}_d^* = u_{da}^* \beta_{af} n_f. \quad (24)$$

The thermoelastic representation formula (19) can be written in contracted notation as:

$$U_D(\xi) = \int_C (U_{DA}^* T_A - \tilde{T}_{DA}^* U_A) dC - \int_R U_{DA}^* S_A dR, \quad (25)$$

The vector  $S_A$  can be written in the split form as follows

$$S_A = S_A^0 + S_A^T + S_A^u + S_A^{\dot{T}} + S_A^{\ddot{T}} + S_A^{\dot{u}} + S_A^{\ddot{u}}, \quad (26)$$

Where

$$S_A^0 = \begin{cases} \rho \omega^2 x_a & a = A = 1, 2, 3; \\ 0 & A = 4, \end{cases} \quad (27)$$

$$S_A^T = \omega_{AF} U_F \quad \text{with} \quad \omega_{AF} = \begin{cases} -D_a & A = 1, 2, 3; F = 4; \\ 0 & \text{otherwise,} \end{cases} \quad (28)$$

$$S_A^u = -(D_{af} + \Lambda D_{a1f}) \bar{U} U_F \quad \text{with} \quad \bar{U} = \begin{cases} 1 & a = A = 1, 2, 3; f = F = 1, 2, 3; \\ 0 & \text{otherwise,} \end{cases} \quad (29)$$

$$S_A^{\dot{T}} = -\rho c (x+1)^m \delta_{AF} \dot{U}_F \quad \text{with} \quad \delta_{AF} = \begin{cases} 1 & A = 4; F = 4; \\ 0 & \text{otherwise,} \end{cases} \quad (30)$$

$$S_A^{\ddot{T}} = -\rho c (x+1)^m \tau_1 \delta_{AF} \ddot{U}_F, \quad (31)$$

$$S_A^{\dot{u}} = -T_0 \dot{A} \delta_{1j} \beta_{fg} \varepsilon \dot{U}_F, \quad (32)$$

$$S_A^{\ddot{u}} = \mathcal{A} \ddot{U}_F \quad \text{with} \quad \mathcal{A} = \begin{cases} \rho & A = 1, 2, 3; F = 1, 2, 3; \\ 0 & A = 4; f = F = 4. \end{cases} \quad (33)$$

The thermoelastic representation formula (19) can also be written in matrix form as follows:

$$[S_A] = \begin{bmatrix} \rho \omega^2 x_a \\ 0 \end{bmatrix} + \begin{bmatrix} -D_a T \\ 0 \end{bmatrix} + \begin{bmatrix} -(D_{af} + \Lambda D_{a1f}) u_f \\ 0 \end{bmatrix} \\ + (\rho c (x+1)^m) \begin{bmatrix} 0 \\ \dot{T} \end{bmatrix} - \rho c (x+1)^m \tau_1 \begin{bmatrix} 0 \\ \ddot{T} \end{bmatrix} - T_0 \begin{bmatrix} 0 \\ \beta_{ab} \dot{u}_{a,b} \end{bmatrix} + \begin{bmatrix} \rho \ddot{u}_a \\ 0 \end{bmatrix}. \quad (34)$$

Our task now is to implement the DRBEM. To transform the domain integral in (25) to the boundary, we approximate the source vector  $S_A$  in the domain as usual by a series of given tensor functions  $f_{AN}^q$  and unknown coefficients  $\alpha_N^q$

$$S_A \approx \sum_{q=1}^N f_{AN}^q \alpha_N^q. \tag{35}$$

According to the DRBEM, the surface of the solid has to be discretized into boundary elements. In order to make the implementation easy to compute, we use  $N_b$  collocation points on the boundary  $\mathcal{C}$  and another  $N_i$  in the interior of  $R$  so that the total number of interpolation points is  $N = N_b + N_i$ .

Thus, the thermoelastic representation formula (25) can be written in the following form

$$U_D(\xi) = \int_{\mathcal{C}} (U_{DA}^* T_A - \tilde{T}_{DA}^* U_A) dC - \sum_{q=1}^N \int_R U_{DA}^* f_{AN}^q dR \alpha_N^q. \tag{36}$$

By applying the WRM to the following inhomogeneous elastic and thermal equations:

$$L_{gb} u_{fn}^q = f_{an}^q, \tag{37}$$

$$L_{ab} T^q = f_{pj}^q, \tag{38}$$

where the weighting functions are chosen to be the elastic and thermal fundamental solutions  $u_{da}^*$  and  $T^*$ . Then the elastic and thermal representation formulae are similar to those of Fahmy [41] within the context of the uncoupled theory and are given as follows

$$u_{de}^q(\xi) = \int_{\mathcal{C}} (u_{da}^* t_{ae}^q - t_{da}^* u_{ae}^q) dC - \int_R u_{da}^* f_{ae}^q dR, \tag{39}$$

$$T^q(\xi) = \int_{\mathcal{C}} (q^* T^q - q^q T^*) dC - \int_R f^q T^* dR. \tag{40}$$

The dual representation formulae of elastic and thermal fields can be combined to form a single equation as follows

$$U_{DN}^q(\xi) = \int_{\mathcal{C}} (U_{DA}^* T_{AN}^q - T_{DA}^* U_{AN}^q) dC - \int_R U_{DA}^* f_{AN}^q dR, \tag{41}$$

with the substitution of (41) into (36), the dual reciprocity representation formula of coupled thermoelasticity can be expressed as follows

$$U_D(\xi) = \int_{\mathcal{C}} (U_{DA}^* T_A - \tilde{T}_{DA}^* U_A) dC + \sum_{q=1}^N \left( U_{DN}^q(\xi) + \int_{\mathcal{C}} (T_{DA}^* U_{AN}^q - U_{DA}^* T_{AN}^q) dC \right) \alpha_N^q. \tag{42}$$

To calculate interior stresses, (42) is differentiated with respect to  $\xi_l$  as follows

$$\begin{aligned} \frac{\partial U_D(\xi)}{\partial \xi_l} = & - \int_{\mathcal{C}} (U_{DA,l}^* T_A - \tilde{T}_{DA,l}^* U_A) dC \\ & + \sum_{q=1}^N \left( \frac{\partial U_{DN}^q(\xi)}{\partial \xi_l} - \int_{\mathcal{C}} (T_{DA,l}^* U_{AN}^q - U_{DA,l}^* T_{AN}^q) dC \right) \alpha_N^q. \end{aligned} \tag{43}$$

According to the steps described in Fahmy [42], the dual reciprocity boundary integral equation (42) can be written in the following system of equations

$$\zeta \check{u} - \eta \check{t} = (\zeta \check{U} - \eta \check{\phi}) \alpha. \tag{44}$$

It is important to note the difference between the matrices  $\zeta$  and  $\check{\zeta}$ : whereas  $\zeta$  contains the fundamental solution  $T_M^*$ , the matrix  $\check{\zeta}$  contains the modified fundamental tensor  $\check{T}_M^*$  with the coupling term.

The technique was proposed by Partridge et al. [43] can be extended to treat the convective terms, then the generalized displacements  $U_F$  and velocities  $\dot{U}_F$  are approximated by a series of tensor functions  $f_{FD}^q$  and unknown coefficients  $\gamma_D^q$  and  $\tilde{\gamma}_D^q$

$$U_F \approx \sum_{q=1}^N f_{FD}^q(x) \gamma_D^q, \tag{45}$$

$$\dot{U}_F \approx \sum_{q=1}^N f_{FD}^q(x) \tilde{\gamma}_D^q, \tag{46}$$

The gradients of the generalized displacement and velocity can be approximated as follows

$$U_{F,g} \approx \sum_{q=1}^N f_{K,g}^q(x) \gamma_K^q, \tag{47}$$

$$\dot{U}_{F,g} \approx \sum_{q=1}^N f_{FD,g}^q(x) \tilde{\gamma}_D^q. \tag{48}$$

These approximations are substituted into equations (28) and (32) to approximate the corresponding source terms as follows

$$S_A^T = \sum_{q=1}^N S_{AD}^{T,q} \gamma_D^q, \tag{49}$$

$$S_A^{\dot{u}} = -T_0 \beta_{fg} \varepsilon \sum_{q=1}^N S_{AD}^{\dot{u},q} \tilde{\gamma}_D^q, \tag{50}$$

where

$$S_{AD}^{T,q} = S_{AF} f_{FD,g}^q, \tag{51}$$

$$S_{AD}^{\dot{u},q} = S_{FA} f_{FD,g}^q. \tag{52}$$

The same point collocation procedure described in Gaul, et al. [44] can be applied to (35), (45) and (46). This leads to the following system of equations

$$\check{S} = J\alpha, \quad U = J'\gamma, \quad \dot{U} = J'\tilde{\gamma}. \tag{53}$$

Similarly, the application of the point collocation procedure to the source terms equations (29), (30), (31), (33), (49) and (50) leads to the following system of equations

$$\check{S}^u = -(D_{af} + \Lambda D_{a1f}) \check{U} U_F \quad \text{with} \quad \check{U} = \begin{cases} 1 & a = A = 1, 2, 3; f = F = 1, 2, 3; \\ 0 & \text{otherwise,} \end{cases} \tag{54}$$

$$\check{S}^T = \rho c (x + 1)^m \delta_{AF} \dot{U}, \tag{55}$$

$$\check{S}^{\dot{u}} = -c \rho (x + 1)^m \tau_1 \delta_{AF} \ddot{U}, \tag{56}$$

$$\check{S}^{\ddot{u}} = \check{A} \ddot{U}, \tag{57}$$

$$\check{S}^T = \mathcal{B}^T \gamma, \tag{58}$$

$$\check{S}^{\dot{u}} = -T_0 \beta_{fg} \varepsilon \mathcal{B}^{\dot{u}} \tilde{\gamma}. \tag{59}$$

Solving the system (53) for  $\alpha$ ,  $\gamma$  and  $\tilde{\gamma}$  yields

$$\alpha = J^{-1} \check{S}, \quad \gamma = J'^{-1} U, \quad \tilde{\gamma} = J'^{-1} \dot{U}, \tag{60}$$

Now, the coefficients  $\alpha$  can be expressed in terms of nodal values of the unknown displacements  $U$ , velocities  $\dot{U}$  and accelerations  $\ddot{U}$  as follows:

$$\alpha = J^{-1} \left( \check{S}^0 + [\mathcal{B}^T J'^{-1} - (D_{af} + \Lambda D_{a1f}) \check{U}] U + \left[ \rho c (x + 1)^m \delta_{AF} - T_0 \beta_{fg} \varepsilon \mathcal{B}^{\dot{u}} J'^{-1} \right] \dot{U} + [\check{A} - \rho c (x + 1)^m \tau_1 \delta_{AF}] \ddot{U} \right), \tag{61}$$

where  $\tilde{A}$  and  $\mathcal{B}^T$  are assembled using the submatrices  $[A]$  and  $\omega_{AF}$  respectively. Substituting from Eq. (61) into Eq. (44), we obtain

$$M\ddot{U} + \Gamma\dot{U} + KU = \mathbb{Q}, \quad (62)$$

in which  $M, \Gamma, K$  and  $\mathbb{Q}$  are independent of time and are defined by

$$\begin{aligned} V &= (\eta\check{\phi} - \zeta\check{U})J^{-1}, & \tilde{M} &= V[\tilde{A} - c\rho(x+1)^m\tau_1\delta_{AF}], \\ \Gamma &= V[\rho c(x+1)^m\delta_{AF} - T_0\beta_{fg}\varepsilon\mathcal{B}^u J'^{-1}], \\ K &= \check{\zeta} + V[\mathcal{B}^T J'^{-1} + (D_{af} + \Lambda D_{a1f})\mathbb{U}], & \mathbb{Q} &= \eta T + V\check{S}^0, \end{aligned} \quad (63)$$

where  $V, M, \Gamma$  and  $K$  represent the volume, mass, damping and stiffness matrices, respectively;  $\ddot{U}, \dot{U}, U$  and  $\mathbb{Q}$  represent the acceleration, velocity, displacement and external force vectors, respectively. The initial value problem consists of finding the function  $U = U(\tau)$  satisfying equation (62) and the initial conditions  $U(0) = U_0, \dot{U}(0) = V_0$  where  $U_0, V_0$  are given vectors of initial data. Then, from Eq. (62), we can compute the initial acceleration vector  $W_0$  as follows

$$MW_0 = \mathbb{Q}_0 - \Gamma V_0 - KU_0. \quad (64)$$

An implicit-explicit time integration algorithm of Hughes et al. [45, 46], was developed and implemented for use with the DRBEM. This algorithm consists of satisfying the following equations

$$M\ddot{U}_{n+1} + \Gamma^I\dot{U}_{n+1} + \Gamma^E\tilde{U}_{n+1} + K^I U_{n+1} + K^E \tilde{U}_{n+1} = \mathbb{Q}_{n+1}, \quad (65)$$

$$U_{n+1} = \tilde{U}_{n+1} + \gamma\Delta\tau^2\dot{U}_{n+1}, \quad (66)$$

$$\dot{U}_{n+1} = \tilde{U}_{n+1} + \alpha\Delta\tau\ddot{U}_{n+1}, \quad (67)$$

Where

$$\tilde{U}_{n+1} = U_{n+1} + \Delta\tau\dot{U}_n + (1 - 2\gamma)\frac{\Delta\tau^2}{2}\ddot{U}_n, \quad (68)$$

$$\tilde{\dot{U}}_{n+1} = \dot{U}_n + (1 - \alpha)\Delta\tau\ddot{U}_n, \quad (69)$$

in which the implicit and explicit parts are respectively denoted by the superscripts  $I$  and  $E$ . Also, we used the quantities  $\tilde{U}_{n+1}$  and  $\tilde{\dot{U}}_{n+1}$  to denote the predictor values, and  $U_{n+1}$  and  $\dot{U}_{n+1}$  to denote the corrector values [45, 46]. It is easy to recognize that the equations (66)-(69) correspond to the Newmark formulas [47].

At each time-step, equations (65)-(69), constitute an algebraic problem in terms of the unknown  $\ddot{U}_{n+1}$ . The first step in the code starts by forming and factoring the effective mass

$$M^* = M + \gamma\Delta\tau C^I + \gamma\Delta\tau^2 K^I. \quad (70)$$

The time step  $\Delta\tau$  must be constant to run this step. As the time-step  $\Delta\tau$  is changed, the first step should be repeated at each new step. The second step is to form residual force

$$\mathbb{Q}_{n+1}^* = \mathbb{Q}_{n+1} - C^I\tilde{\dot{U}}_{n+1} - C^E\tilde{\dot{U}}_{n+1} - K^I\tilde{U}_{n+1} - K^E\tilde{U}_{n+1}. \quad (71)$$

Note that in the implicit part,  $M^*$  is always nonsymmetric. However,  $M^*$  still possesses the usual "band-profile" structure associated with the connectivity of the DRBEM mesh, and has a symmetric profile. So the third step is to solve  $M^*\ddot{U}_{n+1} = \mathbb{Q}_{n+1}^*$  using a Crout elimination algorithm [48] which fully exploits that structure in that zeroes outside the profile are neither stored nor operated upon. The fourth step is to use predictor-corrector equations (66) and (67) to obtain the corrector displacement and velocity vectors, respectively.

The stability analysis of the algorithm under consideration has been discussed in detail in Hughes and Liu [45] and the stability conditions have also been derived in the same reference, therefore does not strictly apply to the considered problem.

#### 4. Numerical Results And Discussion

Following Rasolofosaon and Zinszner [49] monoclinic North Sea sandstone reservoir rock was chosen as an anisotropic material and physical data are as follows:

Elasticity tensor

$$C_{abfg} = \begin{bmatrix} 17.77 & 3.78 & 3.76 & 0.24 & -0.28 & 0.03 \\ 3.78 & 19.45 & 4.13 & 0 & 0 & 1.13 \\ 3.76 & 4.13 & 21.79 & 0 & 0 & 0.38 \\ 0 & 0 & 0 & 8.30 & 0.66 & 0 \\ 0 & 0 & 0 & 0.66 & 7.62 & 0 \\ 0.03 & 1.13 & 0.38 & 0 & 0 & 7.77 \end{bmatrix} \text{GPa} \quad (72)$$

Mechanical temperature coefficient

$$\beta_{ab} = \begin{bmatrix} 0.001 & 0.02 & 0 \\ 0.02 & 0.006 & 0 \\ 0 & 0 & 0.05 \end{bmatrix} \cdot 10^6 \text{N/Km}^2 \quad (73)$$

Tensor of thermal conductivity is

$$k_{ab} = \begin{bmatrix} 1 & 0.1 & 0.2 \\ 0.1 & 1.1 & 0.15 \\ 0.2 & 0.15 & 0.9 \end{bmatrix} \text{W/(mK)} \quad (74)$$

Mass density  $\rho = 2216 \text{ kg/m}^3$  and heat capacity  $c = 0.1 \text{ J/(kg K)}$ ,  $H_0 = 1000000$  Oersted,  $\mu = 0.5$  Gauss/Oersted,  $\mathbf{N} = 2$ ,  $\mathbf{h} = 2$ ,  $\Delta\tau = 0.0001$ . The numerical values of the temperature and displacement are obtained by discretizing the boundary into 120 elements ( $N_b = 120$ ) and choosing 60 well spaced out collocation points ( $N_i = 60$ ) in the interior of the solution domain, refer to the recent work of Fahmy [50-52].

The initial and boundary conditions considered in the calculations are

$$\text{at } \tau = 0 \quad u_1 = u_2 = \dot{u}_1 = \dot{u}_2 = 0, T = 0 \quad (75)$$

$$\text{at } x = 0 \quad \frac{\partial u_1}{\partial x} = \frac{\partial u_2}{\partial x} = 0, \frac{\partial T}{\partial x} = 0 \quad (76)$$

$$\text{at } x = \underline{\gamma} \quad \frac{\partial u_1}{\partial x} = \frac{\partial u_2}{\partial x} = 0, \frac{\partial T}{\partial x} = 0 \quad (77)$$

$$\text{at } y = 0 \quad \frac{\partial u_1}{\partial y} = \frac{\partial u_2}{\partial y} = 0, \frac{\partial T}{\partial y} = 0 \quad (78)$$

$$\text{at } y = \underline{\beta} \quad \frac{\partial u_1}{\partial y} = \frac{\partial u_2}{\partial y} = 0, \frac{\partial T}{\partial y} = 0 \quad (79)$$

The present work should be applicable to any dynamic coupled thermo-elastic deformation problem.

Table 1 shows the variation of the temperature  $T$ , the displacements  $u_1$  and  $u_2$  and thermal stresses  $\sigma_{11}$ ,  $\sigma_{12}$  and  $\sigma_{22}$  with time  $\tau$ . We can conclude from this table that the displacements and thermal stresses increase with increasing  $\tau$  but the temperature  $T$  decreases with increasing  $\tau$ . In the special case under consideration. These results obtained with the DRBEM have been written in the table 1, the validity of the proposed method was examined and confirmed by comparing the obtained results with those obtained in table 2 using the Meshless Local Petrov-Galerkin (MLPG) method of Hosseini et al. [53]. It can be seen from these tables that the DRBEM results are in excellent agreement with the results obtained by MLPG method.

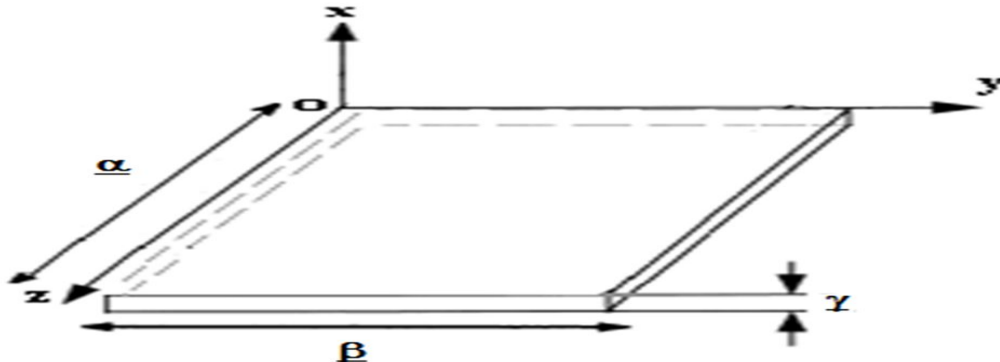


Fig. 1. The coordinate system of the plate.



**Table 1. Variation of the temperature, displacements and thermal stresses with time for DRBEM method**

|     |            |            |             |            |            |             |
|-----|------------|------------|-------------|------------|------------|-------------|
| 0.0 | 1.00000000 | 0.76353454 | -0.78353535 | 0.04578125 | 0.16489345 | -0.59482854 |
| 0.1 | 0.97564321 | 0.77345252 | -0.75434333 | 0.04892613 | 0.21839467 | -0.54293714 |
| 0.2 | 0.94523223 | 0.78455654 | -0.73424244 | 0.05173821 | 0.24485945 | -0.50923845 |
| 0.3 | 0.91254367 | 0.79565787 | -0.70419252 | 0.05347621 | 0.29384673 | -0.46892341 |
| 0.4 | 0.88453923 | 0.80253642 | -0.68343465 | 0.05826364 | 0.33845683 | -0.43928143 |
| 0.5 | 0.85646342 | 0.81343556 | -0.64959587 | 0.06182828 | 0.37693481 | -0.40287456 |
| 0.6 | 0.82436734 | 0.82435678 | -0.61746567 | 0.06372737 | 0.39278476 | -0.37494983 |
| 0.7 | 0.79653245 | 0.83569012 | -0.57564653 | 0.06734242 | 0.42578923 | -0.32658739 |
| 0.8 | 0.76434531 | 0.84563535 | -0.53673213 | 0.07315241 | 0.47283601 | -0.26294879 |
| 0.9 | 0.73456518 | 0.85363627 | -0.46278342 | 0.07593080 | 0.52683246 | -0.23345634 |
| 1.0 | 0.69283829 | 0.86345345 | -0.41632342 | 0.07853454 | 0.55374852 | -0.17659682 |

**Table 2. Variation of the temperature, displacements and thermal stresses with time for MLPG method**

|     |            |            |             |            |            |             |
|-----|------------|------------|-------------|------------|------------|-------------|
| 0.0 | 1.00000000 | 0.76353452 | -0.78353533 | 0.04578123 | 0.16489342 | -0.59482851 |
| 0.1 | 0.97564319 | 0.77345250 | -0.75434331 | 0.04892611 | 0.21839465 | -0.54293712 |
| 0.2 | 0.94523221 | 0.78455651 | -0.73424242 | 0.05173819 | 0.24485943 | -0.50923843 |
| 0.3 | 0.91254365 | 0.79565784 | -0.70419249 | 0.05347620 | 0.29384671 | -0.46892338 |
| 0.4 | 0.88453921 | 0.80253640 | -0.68343462 | 0.05826362 | 0.33845682 | -0.43928140 |
| 0.5 | 0.85646340 | 0.81343553 | -0.64959584 | 0.06182826 | 0.37693480 | -0.40287453 |
| 0.6 | 0.82436732 | 0.82435675 | -0.61746563 | 0.06372735 | 0.39278474 | -0.37494981 |
| 0.7 | 0.79653241 | 0.83569010 | -0.57564651 | 0.06734240 | 0.42578921 | -0.32658737 |
| 0.8 | 0.76434529 | 0.84563533 | -0.53673211 | 0.07315239 | 0.47283600 | -0.26294878 |
| 0.9 | 0.73456516 | 0.85363627 | -0.46278340 | 0.07593077 | 0.52683245 | -0.23345632 |
| 1.0 | 0.69283827 | 0.86345343 | -0.41632340 | 0.07853452 | 0.55374851 | -0.17659680 |

## References

- Biot M. Thermoelasticity and irreversible thermo-dynamics. *J. Appl. Phys.* 1956;27:249-253.
- Duhamel J. Some memoire sur les phenomenes thermo-mechanique. *J. de l'Ecole polytech.* 1837; 15:1-57.
- Neumann F. *Vorlesungen Uber die theorie der elasticitat.* Meyer: Brestau, 1885.
- Lord HW, Shulman Y. A generalized dynamical theory of thermoelasticity. *J. Mech. Phys. Solids.* 1967;15:299-309.
- Green AE, Lindsay KA. Thermoelasticity. *J. Elast.* 1972;2:1-7.
- Green AE and Naghdi PM. On undamped heat waves in an elastic solid. *J. Therm. Stresses.* 15;1992:253-264.
- Green AE and Naghdi PM. Thermoelasticity without energy dissipation. *J. Elast.* 1993;31:189-208.
- El-Naggar AM, Abd-Alla AM, Fahmy MA, Ahmed SM. Thermal stresses in a rotating non-homogeneous orthotropic hollow cylinder, *Heat Mass Transfer.* 2002;39:41-46.
- El-Naggar AM, Abd-Alla AM, Fahmy MA. The propagation of thermal stresses in an infinite elastic slab. *Appl. Math. Comput.* 2004;157:307-312.
- Abd-Alla AM, El-Naggar AM, Fahmy MA, Magneto-thermoelastic problem in non-homogeneous isotropic cylinder. *Heat Mass Transfer.* 2003;39:625-629.
- Abd-Alla AM, Fahmy MA, El-Shahat TM. Magneto-thermo-elastic stresses in inhomogeneous anisotropic solid in the presence of body force. *Far East J. Appl. Math.* 2007;27:499-516.
- Abd-Alla AM, Fahmy MA, El-Shahat TM. Magneto-thermo-elastic problem of a rotating non-homogeneous anisotropic solid cylinder. *Arch. Appl. Mech.* 2008;78:135-148.
- Qin QH. 2D Green's functions of defective magneto-electroelastic solids under thermal loading. *Eng. Anal. Boundary Elem.* 2005;29:577-585.
- Fahmy MA. Effect of initial stress and inhomogeneity on magneto-thermo-elastic stresses in a rotating anisotropic solid. *JP J. Heat Mass Transfer.* 2007;1:93-112.

- Fahmy MA. Thermoelastic stresses in a rotating non-homogeneous anisotropic body. *Numer. Heat Transfer, Part A*. 2008;53:1001-1011.
- Fahmy MA. Thermal stresses in a spherical shell under three thermoelastic models using FDM. *Int. J. Numer. Methods Appl.* 2009;2:123-128.
- Fahmy MA. Finite difference algorithm for transient magneto-thermo-elastic stresses in a non-homogeneous solid cylinder. *Int. J. Mater. Eng. Technol.* 2010;3:87-93.
- Fahmy MA. Influence of inhomogeneity and initial stress on the transient magneto-thermo-visco-elastic stress waves in an anisotropic solid. *World J. Mech.* 2011;1:256-265.
- Fahmy MA. Numerical modeling of transient magneto-thermo-viscoelastic waves in a rotating nonhomogeneous anisotropic solid under initial stress. *Int. J. Model. Simul. Sci. Comput.* 2012;3:125002.
- Fahmy MA, El-Shahat TM. The effect of initial stress and inhomogeneity on the thermoelastic stresses in a rotating anisotropic solid. *Arch. Appl. Mech.* 2008;78:431-442.
- Othman MIA, Song Y. Effect of rotation on plane waves of generalized electro-magneto-thermoviscoelasticity with two relaxation times. *Appl. Math. Modell.* 2008;32: 811–825.
- Othman MIA, Atwa SY, Farouk RM. Generalized magneto-thermoviscoelastic plane waves under the effect of rotation without energy dissipation. *Int. J. Eng. Sci.* 2008;46:639-653.
- Sladek V, Sladek J, Tanaka M, Zhang Ch. Local integral equation method for potential problems in functionally graded anisotropic materials. *Eng. Anal. Boundary Elem.* 2005;29:829-843.
- Hou PF, He S, Chen CP. 2D general solution and fundamental solution for orthotropic thermoelastic materials. *Eng. Anal. Boundary Elem.* 2011;35:56-60.
- Davì G, Milazzo A. A regular variational boundary model for free vibrations of magneto-electro-elastic structures. *Eng. Anal. Boundary Elem.* 2011;35:303-312.
- Espinosa JV, Mediavilla AF. Boundary element method applied to three dimensional thermoelastic contact. *Eng. Anal. Boundary Elem.* 2012;36:928-933.
- Abreu AI, Canelas A, Sensale B, Mansur WJ. CQM-based BEM formulation for uncoupled transient quasistatic thermoelasticity analysis. *Eng. Anal. Boundary Elem.* 2012;36:568-578.
- Skouras ED, Bourantas GC, Loukopoulos VC, Nikiforidis GC. Truly meshless localized type techniques for the steady-state heat conduction problems for isotropic and functionally graded materials. *Eng. Anal. Boundary Elem.* 2011;35:452-464.
- Mojdehi AR, Darvizeh A, Basti A, Rajabi H. Three dimensional static and dynamic analysis of thick functionally graded plates by the meshless local Petrov-Galerkin (MLPG) method. *Eng. Anal. Boundary Elem.* 2011;35:1168-1180.
- Loghman A, Aleayoub SMA, Sadi MH. Time-dependent magnetothermoelastic creep modeling of FGM spheres using method of successive elastic solution. *Appl. Math. Modell.* 2012;36:836-845.
- Mirzaei D, Dehghan M. New implementation of MLBIE method for heat conduction analysis in functionally graded materials. *Eng. Anal. Boundary Elem.* 2012;36:511-519.
- Nardini D, Brebbia CA. A new approach to free vibration analysis using boundary elements, in: C.A. Brebbia (Eds.), *Boundary elements in engineering*, Springer, Berlin, 1982, pp. 312-326.
- Brebbia CA, Telles JCF, Wrobel L. *Boundary element techniques in Engineering*, Springer-Verlag, New York, 1984.
- Wrobel LC, Brebbia CA. The dual reciprocity boundary element formulation for nonlinear diffusion problems. *Comput. Methods Appl. Mech. Eng.* 65 (1987) 147-164.
- Partridge PW, Brebbia CA. Computer implementation of the BEM dual reciprocity method for the solution of general field equations. *Commun. Appl. Numer. Methods.* 1990;6:83-92.
- Partridge PW, Wrobel LC. The dual reciprocity boundary element method for spontaneous ignition. *Int. J. Numer. Methods Eng.* 1990;30:953–963.
- Fahmy MA. Application of DRBEM to non-steady state heat conduction in non-homogeneous anisotropic media under various boundary elements. *Far East J. Math. Sci.* 2010;43:83-93.
- Fahmy MA. A time-stepping DRBEM for magneto-thermo-viscoelastic interactions in a rotating nonhomogeneous anisotropic solid. *Int. J. Appl. Mech.* 2011;3:1-24.
- Fahmy MA. Transient magneto-thermoviscoelastic plane waves in a non-homogeneous anisotropic thick strip subjected to a moving heat source. *Appl. Math. Modell.* 2012;36: 4565-4578.

- Fahmy MA. transient magneto-thermo-viscoelastic stresses in a rotating nonhomogeneous anisotropic solid with and without a moving heat source. *J. Eng. Phys. Thermophys.* 2012;85:874-880.
- Fahmy MA. Transient magneto-thermo-elastic stresses in an anisotropic viscoelastic solid with and without moving heat source, *Numer. Heat Transfer, Part A.* 61 (2012) 547-564.
- Fahmy MA. A time-stepping DRBEM for the transient magneto-thermo-visco-elastic stresses in a rotating non-homogeneous anisotropic solid. *Eng. Anal. Boundary Elem.* 2012;36:335-345.
- Partridge PW, Brebbia CA, Wrobel LC. *The dual reciprocity boundary element method*, Computational Mechanics Publications, Boston, Southampton, 1992.
- Gaul L, Kögl M, Wagner M. *Boundary element methods for engineers and scientists*, Springer-Verlag, Berlin, 2003.
- Hughes TJR, Liu WK. Implicit-Explicit finite element in Transient analysis: Stability theory. *ASME J. Appl. Mech.* 1978;45:371-374.
- Hughes TJR, Liu WK. Implicit-Explicit finite element in Transient analysis: Implementation and numerical examples. *ASME J. Appl. Mech.* 1978;45:375-378.
- Newmark NM. A method of computation for structural dynamics, *J. Eng. Mech. Div.* 1959;85:67-94.
- Taylor RL. Computer procedures for finite element analysis, in: O.C. Zienkiewicz (Third Edition), *The finite element method*, McGraw Hill, London, 1977.
- Rasolofosaon PNJ, Zinszner BE. Comparison between permeability anisotropy and elasticity anisotropy of reservoir rocks. *Geophys.* 2002;67:230-240.
- Fahmy MA. The effect of rotation and inhomogeneity on the transient magneto-thermo-visco-elastic stresses in an anisotropic solid. *ASME J. Appl. Mech.* 2012;79:051015.
- Fahmy MA. A 2-D DRBEM for generalized Magneto-Thermo-Viscoelastic Transient Response of rotating functionally graded anisotropic thick strip. *International Journal of Engineering and Technology Innovation.* 2013;3:70-85,.
- Fahmy MA. A computerized DRBEM model for generalized magneto-thermo-visco-elastic stress waves in functionally graded anisotropic thin film/substrate structures. *Latin American Journal of Solids and Structures.* 2014;11:386-409,.
- Hosseini SM, Sladek J, Sladek V. Meshless local Petrov-Galerkin method for coupled thermoelasticity analysis of a functionally graded thick hollow cylinder. *Eng. Anal. Boundary Elem.* 2011;35:827-835.